$^{13}C-^{1}H$ and $^{13}C-^{13}C$ Spin Couplings in [2′-^{13}C]2′-Deoxyribonucleosides: Correlations with Molecular Structure

Tapasree Bandyopadhyay,[†] Jian Wu,[‡] Wayne A. Stripe,[†] Ian Carmichael,[§] and Anthony S. Serianni*,[†]

Contribution from the Department of Chemistry and Biochemistry, University of Notre Dame, Notre Dame, Indiana 46556, Department of Human Biological Chemistry and Genetics, University of Texas Medical Branch, Galveston, Texas 77555-1157, and Radiation Laboratory, University of Notre Dame, Notre Dame, Indiana 46556

Received May 15, 1996[⊗]

Abstract: 2′-Deoxyribonucleosides (2′-deoxyadenosine (**1**), 2′-deoxycytidine (**2**), thymidine **(3**)) singly enriched with ^{13}C at C2′ have been prepared and used to obtain one-, two-, and three-bond $^{13}C-^{1}H$ and $^{13}C-^{13}C$ spin-coupling constants involving C2′. Coupling data are interpreted with assistance from complementary $^{3}J_{HH}$ data (PSEUROT analysis), furanose structural parameters obtained from molecular orbital calculations, structure-coupling correlations found for J_{CH} and J_{CC} in carbohydrates, and calculated *J* values. Spin couplings in **1**−**3** involving C1′ and C2′ are also compared to corresponding values in ribonucleosides in order to assess the effects of nucleoside structure and conformation on *J* values within the furanose ring. $^{1}J_{C2',H2'R}$ and $^{1}J_{C2',H2'S}$ in **1**−**3** and $^{1}J_{C2',H2'}$ in ribonucleosides depend on C−H bond orientation; $^{1}J_{C1',H1'}$ in **1**−**3** and in ribonucleosides exhibits a similar dependence. The latter couplings appear to be essentially unaffected by *N*-glycoside torsion. $^{1}J_{CC}$ values depend on the number and distribution of electronegative substituents on the C−C fragment. A modified projection curve is proposed to aid in the interpretation of $^{2}J_{C2',H1'}$ values; the presence of *N* substitution at C1′ causes a shift to more negative couplings relative to the *O*-substituted analog. In contrast, $^{2}J_{C1',H2'}$ is essentially unaffected by the same change in the electronegative substituent at C1′. $^{2}J_{CC}$ values within the furanose ring are determined by two coupling pathways; in one case (*i.e.*, $^{2}J_{C1',C3'}$), the observed coupling is shown to be the algebraic sum of the two couplings arising from each pathway. $^{3}J_{CH}$ and $^{3}J_{CC}$ values depend in general on appropriate molecular dihedral angles as expected (Karplus relationships); however, $^{3}J_{C2',H4'}$ values exhibit unexpected behavior, thus suggesting potential limitations in its use as a structural probe.

Introduction

The development of heteronuclear methods in multidimensional NMR spectroscopy has had an enormous impact on the ability to assess the three-dimensional structures of biomolecules in solution.[1] These methods in their simplest forms facilitate the assignment of ^{1}H and/or X-nucleus chemical shifts,[2] and in more advanced forms permit the measurement of X-nucleus relaxation,[3] heteronuclear spin couplings,[4] and homonuclear $^{1}H-^{1}H$ NOEs.[5] The integrated analysis of these varied parameters lies at the core of modern conformational analysis of biomacromolecules via NMR spectroscopy.[6]

An absolute requirement for heteronuclear NMR studies of large molecules is the incorporation of stable isotopes, usually ^{13}C and/or ^{15}N, either selectively or uniformly into the target molecule. Until recently, such enrichment had been practical only for proteins via the use of expression systems sustained on appropriately labeled metabolic precursors (*e.g.*, $^{13}CO_2$, D-[UL-$^{13}C_6$]glucose, [UL-$^{13}C_3$]glycerol, and [$^{13}C_2$]acetate).[7] However, reliable chemical and chemoenzymic methods are now available that permit stable isotopic labeling of DNA and RNA within the sugar and/or base moieties,[8] thus leading to the expectation that heteronuclear $^{13}C-^{1}H$ spin couplings and $^{13}C-^{13}C$ spin couplings will be applied more frequently as structural probes in these biomolecules.

In this investigation, we prepared 2′-deoxyribonucleosides (2′-deoxyadenosine, dA (**1**); 2′-deoxycytidine, dC (**2**); thymidine, T (**3**)) (Chart 1) selectively labeled with ^{13}C at C2′ using methods

* Author to whom correspondence should be addressed.
† Department of Chemistry and Biochemistry, University of Notre Dame.
‡ University of Texas Medical Branch.
§ Radiation Laboratory, University of Notre Dame.
⊗ Abstract published in *Advance ACS Abstracts,* December 15, 1996.
(1) Fesik, S. W.; Zuiderweg, E. R. P. *Q. Rev. Biophys.* **1990**, *23*, 97−131.
(2) (a) Bodenhausen, G.; Ruben, D. J. *Chem. Phys. Lett.* **1980**, *69*, 185−189. (b) Bax, A.; Griffey, R. H.; Hawkins, B. L. *J. Magn. Reson.* **1983**, *55*, 301. (c) Müller, L. *J. Am. Chem. Soc.* **1979**, *101*, 4481−4484. (d) Bax, A.; Summers, M. F. *J. Am. Chem. Soc.* **1986**, *108*, 2093−2094.
(3) (a) Kay, L. E.; Torchia, D.; Bax, A. *Biochemistry* **1989**, *28*, 8972−8979. (b) Peng, J. W.; Wagner, G. *J. Magn. Reson.* **1992**, *98*, 308−332. (c) Nirmala, N. R.; Wagner, G. *J. Am. Chem. Soc.* **1988**, *110*, 7557−7558. (d) Kay, L. E.; Bull, T. E.; Nicholson, L. K.; Griesinger, C.; Schwalbe, H.; Bax, A.; Torchia, D. A. *J. Magn. Reson.* **1992**, *100*, 538−558.
(4) Biamonti, C.; Rios, C. B.; Lyons, B. A.; Montelione, G. T. *Adv. Biophys. Chem.* **1994**, *4*, 51−120.
(5) (a) Fesik, S. W.; Zuiderweg, E. R. P. *J. Magn. Reson.* **1988**, *78*, 588−593. (b) Marion, D.; Kay, L. E.; Sparks, S. W.; Torchia, D. A.; Bax, A. *J. Am. Chem. Soc.* **1989**, *111*, 1515−1517.
(6) Wüthrich, K. *NMR of Proteins and Nucleic Acids*, J. Wiley and Sons: New York, 1986.
(7) Muchmore, D. C.; McIntosh, L. P.; Russell, C. B.; Anderson, D. E.; Dahlquist, F. W. *Methods Enzymol.* **1989**, *177*, 44−73.
(8) (a) Nikonowicz, E. P.; Sirr, A.; Legault, P.; Jucker, F. M.; Baer, L. M.; Pardi, A. *Nucl. Acids Res.* **1992**, *20*, 4507−4513. (b) Lancelot, G.; Chanteloup, L.; Beau, J.-M.; Thuong, N. T. *J. Am. Chem. Soc.* **1993**, *115*, 1599−1600. (c) Michnicka, M. J.; Harper, J. W.; King, G. C. *Biochemistry* **1993**, *32*, 395−400. (d) Tate, S.; Ono, A.; Kainosho, M. *J. Am. Chem. Soc.* **1994**, *116*, 5977−5978. (e) Wu, J.; Serianni, A. S. *Biopolymers* **1994**, *34*, 1175−1186. (f) SantaLucia, J., Jr.; Shen, L. X.; Cai, Z.; Lewis, H.; Tinoco, I., Jr. *Nucl. Acids Res.* **1995**, *23*, 4913−4921.
(9) (a) Bandyopadhyay, T.; Wu, J.; Serianni, A. S. *J. Org. Chem.* **1993**, *58*, 5513−5517. (b) Kline, P. C.; Serianni, A. S. *Magn. Reson. Chem.* **1990**, *28*, 324−330.

S0002-7863(96)01622-8 CCC: $14.00

Chart 1

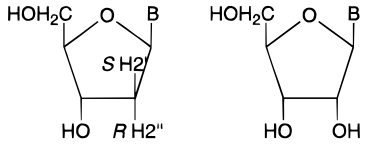

1 B = adenine
2 B = cytosine
3 B = thymine

4 B = adenine
5 B = cytosine
6 B = guanine
7 B = uracil

described previously.[9] Our aim was to measure $^{13}C-^{1}H$ and $^{13}C-^{13}C$ spin couplings (magnitudes and signs) involving C2′ across one, two, and three bonds and to compare these couplings with those involving C1′[9a] and with related couplings in ribonucleosides **4**−**7** (Chart 1)[10] in order to improve the structural interpretation of J_{CH} and J_{CC} values within the furanose ring. Several couplings across the *N*-glycoside linkage in **1**−**7** are also discussed.

Experimental Section

Synthesis of [^{13}C]-Labeled 2′-Deoxyribonucleosides 1−3. The 2′-deoxyribonucleosides **1**−**3** selectively labeled with ^{13}C at C2′ were prepared from the corresponding [2′-^{13}C]ribonucleosides via Barton deoxygenation.[9,11] The [2′-^{13}C]ribonucleoside precursors were prepared from D-[2-^{13}C]ribose and appropriately protected nitrogen bases via Friedel−Krafts (Vorbrüggen) chemistry.[10,12]

NMR Spectroscopy. 1D ^{1}H NMR spectra of aqueous ($^{2}H_2O$) solutions of [2′-^{13}C]**1**−**3** (∼15 mM) were obtained on a Varian VXR-500S (UNITY) FT-NMR spectrometer operating at 499.843 MHz for ^{1}H. ^{1}H-Decoupled ^{13}C NMR spectra of [2′-^{13}C]**1**−**3** were obtained on $^{2}H_2O$ solutions (15−20 mM) on the same spectrometer operating at 125.705 MHz for ^{13}C. Spectra were obtained in 5-mm tubes at 25 °C.

2D ^{1}H−^{1}H TOCSY spectra[13a] of [2′-^{13}C]**1**−**3** (10−15 mM, $^{2}H_2O$) were obtained on a Varian Unity*Plus* 600 FT-NMR spectrometer (Department of Chemistry, Purdue University) operating at 599.944 MHz for ^{1}H. Initial data were collected as a 2048 (F_2) × 256 (F_1) matrix and both dimensions were zero-filled to obtain a final 4K × 4K data set. Sine-bell functions were applied in both dimensions prior to fourier transformation. The mixing time in the TOCSY pulse sequence was set at 100−120 ms. Coupling signs were determined from the inspection of relative cross peak displacements observed in TOCSY spectra, as described previously.[4,13b,c]

Ab Initio Molecular Orbital Calculations and Calculations of Coupling Constants. *Ab initio* molecular orbital calculations on β-D-ribofuranose, conducted using a modified version of the Gaussian 92 suite of programs,[14] have been described previously.[15a] Ten envelope (E) forms and the planar form of this furanose were optimized at the HF/6−31G* level of theory using one set of exocyclic C−O and C−C torsion angles.[15a] Computed structural parameters were used to determine correlations between furanose ring conformation and specific molecular torsion angles that are relevant to the interpretation of $^{3}J_{CH}$ and $^{3}J_{CC}$ values within the ring. A similar treatment was also applied to 2-deoxy-β-D-*erythro*-pentofuranose (2-deoxy-β-D-ribofuranose) using the same C1−O1, C3−O3, C4−C5 and C5−O5 bond torsions used for β-D-ribofuranose;[15a] only results appropriate to the present study are discussed herein, and a more complete account will be presented elsewhere.

$^{2}J_{C1,H2}$ and $^{2}J_{C2,H1}$ values in the E_2 (north) form of methyl β-D-erythrofuranoside **8** and erythrouridine **9** were computed in order to

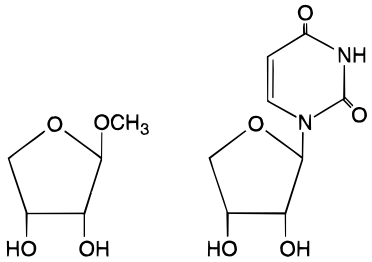

8 **9**

examine the effect of *O*- vs *N*-substitution on $^{2}J_{C1,H2}$ and $^{2}J_{C2,H1}$ values in aldofuranosyl rings. Structures were optimized at the HF/3-21G level of theory, with the C3−C4−O4−C1 endocyclic torsion angle within the furanose ring fixed at 0° to constrain the calculation to the E_2 conformation.[15ab,16a] The optimized H2−C2−O2−H and H3−C3−O3−H torsion angles in **8** and **9** were −51.4° and −157.5°, and −41.8° and −155.3°, respectively. These computations are expected to yield structural parameters sufficient for predicting reliable *trends* in J_{CH} values. Coupling constants were calculated at the HF level employing a basis set [5s2p1d|2s] shown previously to be adequate for the recovery of $^{13}C-^{13}C$[17] and $^{13}C-^{1}H$[16a] spin-coupling constants. Double finite (Fermi-contact) field perturbation theory[16b] was used as before and the computed energy shifts converted to *J* values in the usual manner.

Results and Discussion

A. General Considerations. The conformational flexibility of aldofuranosyl rings (*i.e.*, pseudorotation[18]) complicates the analysis of spin couplings in these structures.[19] In the following discussion, we adopt a comparative approach to the interpretation of J_{CH} and J_{CC} values. Trends in a given $J_{C2',H}$ or $J_{C2',C}$ value within **1**−**3** are compared to those observed for related couplings in ribonucleosides **4**−**7** (Chart 1).[10] Structural conclusions drawn from these comparisons are subsequently tested and/or extended by examining $^{13}C-^{1}H$ and $^{13}C-^{13}C$ couplings involving other carbons in both series of nucleosides. Structural conclusions and conformational models based on J_{CH} and J_{CC} values are then compared to those based on vicinal $^{1}H-^{1}H$ spin couplings ($^{3}J_{HH}$) in **1**−**3** and **4**−**7** which suggest that the former in general prefer south (S; *e.g.*, ^{2}E) conformations more than the latter, and that purine nucleosides show a greater preference for S forms than pyrimidine nucleosides within both series[20] (Table 1). These latter conclusions are based on standard treatments of $^{3}J_{HH}$ data in **1**−**7** using the PSEUROT 6.2 program[21] or empirical methods[22] which assume that the solution behavior of nucleosides is adequately described by a two-state north/south (N/S) model.[23]

(10) Kline, P. C.; Serianni, A. S. *J. Am. Chem. Soc.* **1990**, *112*, 7373−7381.
(11) Robins, M. J.; Wilson, J. S.; Hansske, F. *J. Am. Chem. Soc.* **1983**, *105*, 4059−4065.
(12) Vorbrüggen, H.; Krolikiewicz, K.; Bennua, B. *Chem. Ber.* **1981**, *114*, 1234−1255.
(13) (a) Braunschweiler, L.; Ernst, R. R. *J. Magn. Reson.* **1983**, *53*, 521−528. (b) Serianni, A. S.; Podlasek, C. A. *Carbohydr. Res.* **1994**, *259*, 277−282. (c) Wu, J.; Serianni, A. S. *Carbohydr. Res.* **1992**, *226*, 209−219.
(14) Frisch, M. J.; Trucks, G. W.; Head-Gordon, M.; Gill, P. M. W.; Wong, M. W.; Foresman, J. B.; Johnson, B. G.; Schlegel, H. B.; Robb, M. A.; Replogle, E. S.; Gomperts, R.; Andres, J. L.; Raghavachari, K.; Binkley, J. S.; Gonzales, C.; Martin, R. L.; Fox, D. J.; DeFrees, D. J.; Baker, J.; Stewart, J. J. P.; Pople, J. A. Gaussian 92, Revision C.3; Gaussian, Inc.: Pittsburgh, PA, 1992.
(15) (a) Podlasek, C. A.; Stripe, W. A.; Carmichael, I.; Shang, M.; Basu, B.; Serianni, A. S. *J. Am. Chem. Soc.* **1996**, *118*, 1413−1425. (b) Serianni, A. S.; Chipman, D. M. *J. Am. Chem. Soc.* **1987**, *109*, 5297−5303.
(16) (a) Serianni, A. S.; Wu, J.; Carmichael, I. *J. Am. Chem. Soc.* **1995**, *117*, 8645−8650. (b) Kowalewski, J.; Laaksonen, A.; Roos, B.; Siegbahn, P. *J. Chem. Phys.* **1979**, *71*, 2896−2902.
(17) Carmichael, I. *J. Phys. Chem.* **1993**, *97*, 1789−1792.
(18) Altona, C.; Sundaralingam, M. *J. Am. Chem. Soc.* **1972**, *94*, 8205−8212.
(19) Jardetzky, O. *Biochim. Biophys. Acta* **1980**, *621*, 227−232.
(20) Saenger, W. *Principles of Nucleic Acid Structure*, Springer-Verlag: New York, 1984, p 61.
(21) (a) PSEUROT 6.2, Gorlaeus Laboratories, University of Leiden. (b) de Leeuw, F. A. A. M.; Altona, C. *J. Comp. Chem.* **1983**, *4*, 428−437. (c) Haasnoot, C. A. G.; de Leeuw, F. A. A. M.; de Leeuw, H. P. M.; Altona, C. *Org. Magn. Reson.* **1981**, *15*, 43−52.
(22) (a) Davies, D. B.; Danyluk, S. S. *Biochemistry* **1974**, *13*, 4417−4434. (b) Rinkel, L. J.; Altona, C. *J. Biomol. Struct. Dyn.* **1987**, *4*, 621−649.

Table 1. ^{1}H−^{1}H Spin Couplings[a] in 2′-Deoxyribonucleosides **1**−**3**,[b] Ribonucleosides **4**−**7**,[c] and Methyl β-D-Ribofuranoside **10**[c] and Pseudorotational Analysis by PSEUROT[d]

coupled nuclei	compound							
	1	**2**	**3**	**4**	**5**	**6**	**7**	**10**
H1′, H2′				6.2	4.0	6.0	4.5	1.2
H1′, H2′*R*	6.3	∼6.5	6.8					
H1′, H2′*S*	7.7	∼6.7	6.7					
H2′, H3′				5.3	5.2	5.4	5.3	4.6
H2′*R*, H2′*S*	−14.1	−14.2	−14.2					
H2′*R*, H3′	3.3	4.1	4.1					
H2′*S*, H3′	6.1	∼6.7	6.7					
H3′, H4′	∼3.1	∼4.0	3.9	3.3	6.0	3.6	5.5	6.9
H4′, H5′*R*	4.3	5.3	5.2	3.5	4.3	4.0	4.4	6.6
H4′, H5′*S*	3.3	3.6	3.9	2.8	2.8	3.1	2.9	3.1
H5′*R*, H5′*S*	−12.7	−12.5	−12.5	−12.8	−12.8	−12.8	−12.8	−12.2
P(N)	10[e]	10[e]		23	26	23	40	−7
P(S)	156	146		160	152	155	173	187
τ_m(N)	35[e]	35[e]		32	34	30	36	36[e]
τ_m(S)	34	31		31	34	32	32	36[e]
% S	71	63		70	37	66	42	12
rms error	0.047	0.136		0.002	0.001	0.001	0.000	0.058
% S[f]	71	59		65	40	63	45	

[a] Couplings are reported in Hz, ±0.1 Hz unless otherwise indicated. [b] Data for **1**−**3** were taken from ref 9a. [c] Data for **4**−**7** and **10** were taken from ref 10. [d] $^3J_{HH}$ analysis was performed with PSEUROT 6.2; a copy of the program can be obtained from Gorlaeus Laboratories[21a]. [e] Values held constant in the PSEUROT calculation. [f] Computed from ∑1′ and ∑2″ as described previously for **1** and **2**;[22a] or from $^3J_{H1′,H2′}$ and $^3J_{H3′,H4′}$ for **4**−**7**.[22b]

B. One-Bond ^{13}C−^{1}H Spin Couplings. One-bond ^{13}C−^{1}H spin coupling in aldofuranosyl rings has been shown to depend largely on C−H bond orientation (*i.e.*, quasiaxial vs quasiequatorial),[15a,16a,24] and the behavior of $^1J_{C2′,H2′R}$ and $^1J_{C2′,H2′S}$ in **1**−**3** confirms this dependence. $^1J_{C2′,H2′R}$ is larger than $^1J_{C2′,H2′S}$ in **1**−**3** (Table 2), indicating a preferred quasiequatorial orientation of the C2′−H2′*R* bond and a preferred quasiaxial orientation of the C2′−H2′*S* bond. This relative disposition of bonds is observed in S forms (*e.g.*, ^{2}E). A preference for S forms by **1**−**3** is also suggested from $^3J_{HH}$ analysis (Table 1). Furthermore, the slightly greater preference for S forms by **1** (compared to **2**) (Table 1) is reflected in a greater *difference* (Δ) between $^1J_{C2′,H2′R}$ and $^1J_{C2′,H2′S}$ in this compound (Δ = 3.3 Hz in **1**, Δ = 2.1 Hz in **2**; Table 2).

$^1J_{C2′,H2′}$ values in the purine ribonucleosides **4** and **6** (150.3 ± 0.3 Hz) are smaller than $^1J_{C2′,H2′}$ values in the pyrimidine ribonucleosides **5** and **7** (153.1 ± 0.5 Hz) (Table 2), indicating a greater preference for N forms in the latter in which the C2′−H2′ bond is quasiequatorial or near-quasiequatorial. This conclusion is consistent with $^3J_{HH}$ data (Table 1). Interestingly, $^1J_{C1′,H1′}$ values are also smaller in **4** and **6** (165.6 Hz) than in **5** and **7** (170.2 ± 0.1 Hz), which indicates that a quasiequatorial orientation of the C1′−H1′ bond is more preferred in the latter (*i.e.*, greater preference for N forms). These results suggest that *N*-glycoside torsion may not be as critical as C1′−H1′ bond length/orientation in affecting the $^1J_{C1′,H1′}$ magnitude in nucleosides.[10,25ab] Support for this assertion was obtained from computed $^1J_{C1′,H1′}$ values in **9** in which the furanose was constrained to an E_2 conformation (thus removing C1′−H1′ bond orientation as a factor in affecting coupling magnitude) and the C2′−C1′−N1−C2 torsion angle was varied. Rotation of the latter torsion from 67.9° (optimized value) (*anti* conformation, *ap*) to 180° (torsion held constant in the calculation) (*syn* conformation, high anti, *-sc*) resulted in a small change (0.8 Hz) in $^1J_{C1′,H1′}$ (in these computations all geometric parameters were optimized except for the C3−C4−O4−C1 endocyclic torsion, and the C2′−C1′−N1−C2 torsion (180°) in the latter structure). Previously Davies *et al.*[25a,b] reported a strong dependence of $^1J_{C1′,H1′}$ on *N*-glycoside torsion in nucleosides based on a study of several conformationally constrained molecules. The present results, however, do not support these earlier claims, but instead point to sugar conformation as the major determinant of $^1J_{C1′,H1′}$ in nucleosides.

$^1J_{C2′,H2′}$ values in **4**−**7** are also substantially larger (151.7 ± 1.6 Hz) than corresponding $^1J_{C2′,H2′S}$ values in **1** and **2** (133.5 ± 0.3 Hz), indicating that the loss of an electronegative substituent on the coupled carbon reduces $^1J_{CH}$ values substantially.

Table 2. ^{13}C−^{1}H and ^{13}C−^{13}C Spin Couplings[a] in 2′-Deoxyribonucleosides **1**−**3**,[b] Ribonucleosides **4**−**7**,[c] and Methyl β-D-Ribofuranoside **10**[c]

coupled nuclei	compound							
	1	**2**	**3**	**4**	**5**	**6**	**7**	**10**[d]
C2′, H1′	0	0	0	−3.2	−3.5	−3.3	−3.1	−1.0
C2′, H2′				150.1	153.4	150.5	152.7	
C2′, H2′*R*	136.6	135.8	134.7[f]					
C2′, H2′*S*	133.3	133.7	134.7[f]					
C2′, H3′	0	0	0	0	0	0	0	1.4
C2′, H4′	0.9	1.1	1.1	1.6	1.1	1.6	1.3	0.7
C2′, C1′	36.6	37.0	37.2	42.5	42.9	42.9	43.0	46.7
C2′, C3′	35.5	35.5	35.7	37.9	37.8	37.8	37.8	37.2
C2′, C4′	0	0	0	0.9	0.4	1.0	0.9	br
C2′, C5′	0	1.3	1.3	0	1.6	0	1.6	1.5
C2′, C2		br[e]	0	0	0	0	0	
C2′, C4				0	0	0	0	
C2′, C6		br	1.0	0	0	0	br	
C2′, C8	1.1			0		0		
C1′, H1′	167.4	170.8	170.1	165.6	170.3	165.6	170.1	174.2
C1′, H2′				−3.2	−1.7	∼ −2.9	−2.1	0
C1′, H2′*R*	∼0.4	0	∼0					
C1′, H2′*S*	∼ −5.7	−5.7	∼ −5.7					
C1′, H3′	5.3	4.5	4.6	∼ 5.1	3.0	∼ 4.7	3.5	0.9
C1′, H4′	2.9	2.4	2.2	1.3	0.6	1.3	0.7	3.0
C1′, H6		2.9	2.8		2.8		2.7	
C1′, H8				br		br		
C1′, C3′	0.8			3.3	3.8	3.7	3.8	3.1
C1′, C4′	1.5			0.8	0.8	br	0.9	br
C1′, C5′	0.8			1.8	1.5	0	1.5	br
C1′, C2				0	1.3	0	1.9	
C1′, C4	0.9			0	0	0	0	
C1′, C5	2.8				1.4		1.4	
C1′, C6				0	0.7	0	0.4	
C1′, C8	2.3			1.8		0		

[a] Couplings are reported in Hz, ±0.1 Hz unless otherwise indicated. [b] $J_{C1′,H}$ data were taken from reference 9a; $J_{C2′,H}$ and $J_{C2′,C}$ data were obtained in this study. [c] Data for **4**−**7** and **10** were taken from reference 10. [d] All couplings in **10** correspond to unprimed atoms (*i.e.*, C2′, H1′ = C2, H1; C1′, H1′ = C1, H1 and so forth). [e] Br denotes *br*oadened signal. [f] The non-first-order behavior of the H2′*R*/H2′*S* signals in **3** yields a single value for these couplings which probably represents an average of two dissimilar ^1J values, as observed in **1** and **2**.

C. Two-Bond ^{13}C−^{1}H Spin Couplings. Two-bond coupling between C2′ and H1′ in **1**−**3** is small (Table 2), whereas $^2J_{C2′,H1′}$ is −3.3 ± 0.2 Hz in ribonucleosides **4**−**7** (Table 2). The projection rule,[25c] which predicts $^2J_{CH}$ magnitude and sign in carbohydrates, indicates that $^2J_{C2′,H1′}$ values in north (E_2) and south (^{2}E) forms of **1**−**3** and **4**−**7** will be similar (Chart 2). Thus, differences in conformational equilibria are not expected

(23) This model assumes rapid exchange between generalized north (N) and south (S) conformers. For the β-D-ribofuranosyl and 2-deoxy-β-D-*erythro*-pentofuranosyl rings, the N and S forms are located near the ^{3}E (C3′-*endo*) and ^{2}E (C2′-*endo*) regions of the pseudorotational itinerary, respectively.[18]

(24) Serianni, A. S. In *NMR of Biological Macromolecules*; Stassinopoulou, C., Ed.; NATO ASI Series H: Cell Biology; Springer-Verlag: New York, 1994; Vol. 87, pp 293−306.

(25) (a) Davies, D. B.; MacCoss, M.; Danyluk, S. S. *J. Chem. Soc., Chem. Commun.* **1984**, 536−538. (b) Davies, D. B.; Rajani, P.; Sadikot, H. *J. Chem. Soc., Perkin Trans. 2* **1985**, 279−285. (c) Bock, K.; Pedersen, C. *Acta Chem. Scand. Ser. B* **1977**, *B31*, 354−358.

Chart 2

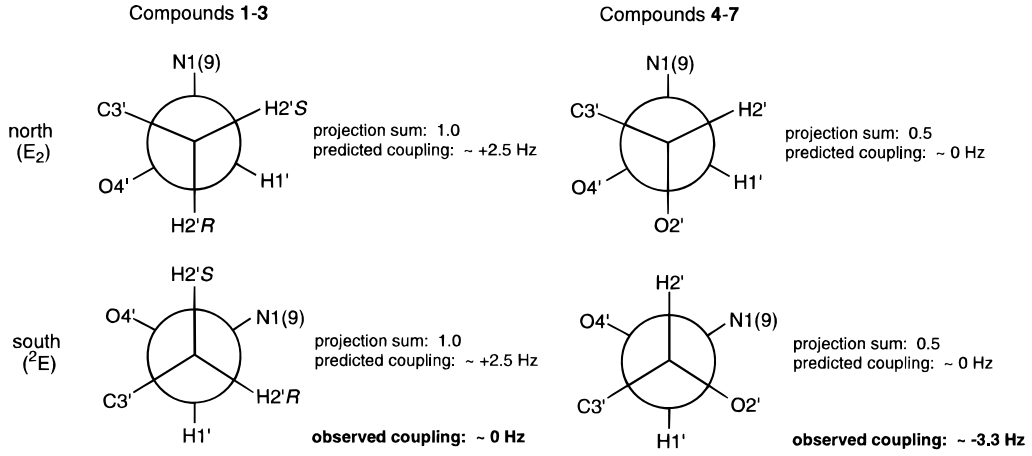

to significantly affect $^2J_{C2',H1'}$ values within either series if a simple two-state N/S model is assumed.

The projection rule[25c] predicts a positive $^2J_{C2',H1'}$ in **1**−**3** (∼2.5 Hz) and a zero value for $^2J_{C2',H1'}$ in **4**−**7**, but zero and negative values, respectively, are observed (Chart 2, Table 2). The projection rule as originally formulated is thus inappropriate for the quantitative prediction of $^2J_{C2',H1'}$ in nucleosides, as noted in a recent study,[15a] presumably because it was developed only for oxygen electronegative substituents along the C−C−H coupling pathway. Indeed, $^2J_{C2,H1} = -1.0$ Hz in the simple *O*-glycoside, methyl *β*-D-ribofuranoside (**10**) (Table 2), is in

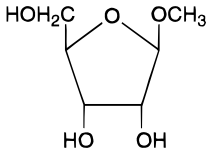

10

better agreement with the projection rule prediction of zero coupling. $^2J_{C2',H1'}$ data for **1**−**7** suggest that nitrogen substitution *on the carbon bearing the coupled proton* causes a shift toward more negative (less positive) couplings relative to the oxygen-substituted analog.

The effect of electronegative substitution on a C−C−H coupling fragment may also originate at the coupled carbon, and may be evaluated through a comparison of $^2J_{C1',H2'}$ values in **1**−**7** and **10**. In **4**, $^2J_{C1',H2'} = -3.2$ Hz, whereas in **10**, $^2J_{C1,H2} = \sim 0$ Hz (Table 2). A PSEUROT analysis of $^3J_{HH}$ values in **10** yields an N/S ratio of 88/12 (Table 1), and the projection rule[25c] predicts standard values of ∼+2.0 and ∼−6.0 Hz for the N and S conformers, respectively. This N/S ratio and the standard couplings yield a small predicted value of $^2J_{C1,H2}$ in **10** (J_{obs} = 0.88 (+2.0) + 0.12 (−6.0) = +1.0 Hz), in fair agreement with the observed behavior. The same standard $^2J_{CH}$ values and an observed −3.2 Hz coupling in **4** yield a 35/65 N/S ratio, in good agreement with the 30/70 and 35/65 ratios obtained from $^3J_{HH}$ analysis (Table 1). The value of $^2J_{C1',H2'}$ in **5** (−1.7 Hz) yields an N/S ratio of 54/46, in fair agreement with the 63/37 and 60/40 ratios obtained by $^3J_{HH}$ analysis (Table 1). In **1**, $^2J_{C1',H2'S} = \sim -5.7$ Hz, and the projection rule gives standard N and S values of approximately 0 and −8 Hz, respectively. These data yield an N/S ratio of 29/71, in good agreement with that obtained by $^3J_{HH}$ analysis (29/71, Table 1). Thus, these results, while limited in scope and subject to some error, suggest that a change from *O*- to *N*-substitution *at the coupled carbon* does not affect $^2J_{CCH}$ values significantly, in contrast to observations made *at the carbon bearing the coupled proton* (see above).

The above conclusions regarding *N*-substitution effects on $^2J_{CH}$ values were tested by comparing $^2J_{C1,H2}$ in methyl α-D-glucopyranoside (**11**) (+1.0 Hz)[26] and 2-acetamido-2-deoxy-α-D-glucopyranose (**12**) (−3.0 Hz).[27] Since ring conformation

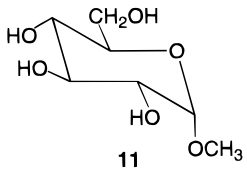

11

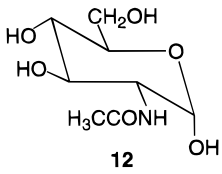

12

is essentially conserved in these two compounds (*i.e.*, $^4C_1$ chair form) and since the substituents at C1 (−OH and −OCH_3) are similar, the different $^2J_{C1,H2}$ values in **11** and **12** can be attributed to the different electronegative substituents at C-2. The data indicate a shift to more negative values in the *N*-substituted compound, in agreement with the nucleoside coupling data. Interestingly, a similar comparison between methyl *β*-D-glucopyranoside (**13**) and 2-acetamido-2-deoxy-*β*-D-glucopyranose (**14**) shows a smaller change in $^2J_{C1,H2}$ (−6.3 to −7.4 Hz), again

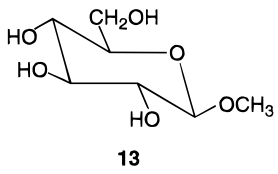

13

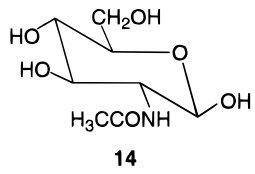

14

more negative in the *N*-substituted compound but suggesting that configuration along the coupling pathway, and perhaps other unidentified structural factors, may influence the *magnitude* of the negative shift. It should also be appreciated that the C−C−H coupling pathways and type of *N*-substitution in **12** and **14** are imprecise mimics of those found in **4**−**7**, thus rendering the conclusions drawn from these comparisons semiquantitative.

The above-noted effect of electronegative substitution at C1′ of aldofuranoses on $^2J_{C1,H2}$ and $^2J_{C2,H1}$ values was also examined by calculating these couplings in two model compounds, methyl *β*-D-erythrofuranoside **8**[28] and erythrouridine **9**.[29a] Computations

(26) Podlasek, C. A.; Wu, J.; Stripe, W. A.; Bondo, P. B.; Serianni, A. S. *J. Am. Chem. Soc.* **1995**, *117*, 8635−8644.
(27) Walker, T. E.; London, R. E.; Barker, R.; Matwiyoff, N. A. *Carbohydr. Res.* **1978**, *60*, 9−18.
(28) Serianni, A. S.; Barker, R. *J. Org. Chem.* **1984**, *49*, 3292−3300.
(29) (a) Kline, P. C.; Serianni, A. S. *J. Org. Chem.* **1992**, *57*, 1772−1777. (b) Lemieux, R. U. *Pure Appl. Chem.* **1971**, *25*, 527−548.

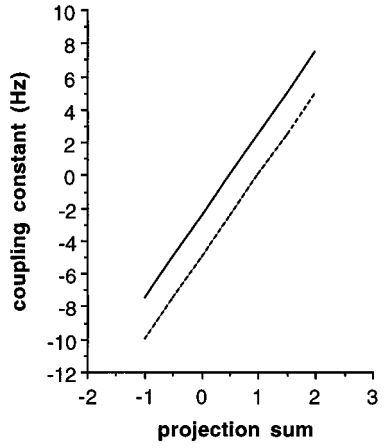

Figure 1. Correlation between $^2J_{CCH}$ magnitude and sign, and projection sum, using the method of Bock and Pederson.[25c] The solid line represents the original correlation for C−C−H coupling pathways containing oxygen substituents; the dashed line represents the modified correlation for the interpretation of $^2J_{C2',H1'}$ values in nucleosides. The latter correlation compensates for *N*-substitution at the carbon bearing the coupled proton.

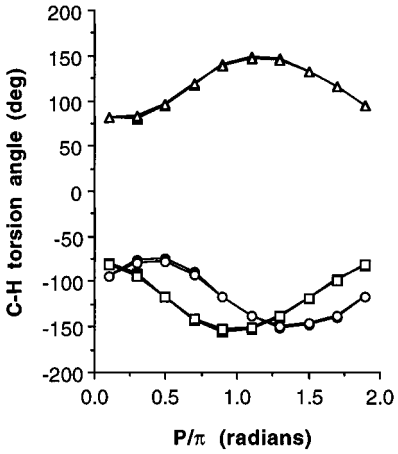

Figure 2. Correlation between furanose ring conformation and endocyclic C−H torsion angles derived from *ab initio* molecular orbital calculations on β-D-ribofuranose and 2-deoxy-β-D-ribofuranose. Solid squares, C1−H3 *ribo*; solid circles, C1−H4 *ribo*; solid triangles, C2−H4 *ribo*; open squares, C1−H3 deoxy*ribo*; open circles, C1−H4 deoxy*ribo*; open triangles, C2−H4 deoxy*ribo*.

were conducted with the furanose ring in an E_2 (N) conformation in both compounds; in this form, the substituents at C1 and C2 are quasiaxial, thereby preventing potential interactions (*e.g.*, intramolecular H bonding) which could complicate the interpretation of results. In **8**, the optimized H1−C1−O1−CH_3 torsion angle was 63.7° (exoanomeric effect[29b]), and in **9** the optimized C2′−C1′−N1−C2 torsion angle was 67.9° (*anti* conformation). In the *O*-glycoside **8**, $^2J_{C1,H2\ (calc)} = -3.3$ Hz and $^2J_{C2,H1\ (calc)} = -5.8$ Hz; the corresponding calculated couplings in the *N*-glycoside **9** were −3.8 and −8.0 Hz. Thus, $^2J_{C1,H2(calc)}$ values differed only slightly (0.5 Hz), whereas $^2J_{C2,H1(calc)}$ values differed by 2.2 Hz; in both cases the *N*-glycoside exhibited a more negative coupling. These results confirm the trend toward more negative coupling in the *N*-substituted compound, with a significantly greater effect observed when the *N*-substitution occurs at the carbon bearing the coupled proton. It should be noted that, due to the molecular size of **8** and **9**, the *ab initio* evaluations of spin coupling constants were made only at the HF level of theory. These calculations are known to exaggerate the magnitude of the two-bond interaction. However, even after appropriate correlation corrections, we expect the above trends to be maintained.

Based on the above considerations, a modified projection curve appropriate for the interpretation of $^2J_{C2',H1'}$ in nucleosides **1**−**7** is proposed in Figure 1. The curve is displaced slightly downward (−2.5 Hz) relative to that for OH-substituted C−C−H pathways to account for the shift to more negative couplings for a given projection sum when nitrogen is present *on the carbon bearing the coupled proton*. Present coupling data do not indicate a need for a modified projection curve for $^2J_{C1',H2'}$ in **1**−**7**, although a downward displacement, albeit considerably smaller, may also be appropriate in this case.

Coupling between C2′ and H3′ in **1**−**3** is small or zero, and similar behavior is observed in **4**−**7**[10] (Table 2). However, the structural interpretation of these couplings differs in both series of compounds. In **1**−**3**, $^2J_{C2',H3'}$ should be very small in *both* N and S forms, and therefore will be insensitive to two-state N/S conformational averaging. In contrast, $^2J_{C2',H3'}$ in ribonucleosides **4**−**7** is predicted to be ∼+3 Hz in N forms and ∼−2 Hz in S forms,[15] and thus the small value of $^2J_{C2',H3'}$ observed in **4**−**7** is attributed to N/S conformational averaging in solution.

D. Three-Bond ^{13}C−^{1}H Spin Couplings. $^3J_{C2',H4'}$ values range from 0.9 to 1.1 Hz in **1**−**3** and from 1.1 to 1.6 Hz in **4**−**7** (Table 2). This coupling is expected to depend on the C2′−C3′−C4′−H4′ dihedral angle, which increases from ∼80° in ^{3}E to ∼140° in ^{2}E forms (Figure 2). Thus $^3J_{C2',H4'}$ should increase as the N/S equilibrium shifts toward S forms if standard Karplus behavior is assumed for this coupling pathway. However, $^3J_{C2',H4'}$ values in **1**−**10** display internally inconsistent behavior. For example, the small $^3J_{C2,H4}$ in **10** (0.7 Hz, Table 2) suggests a greater preference for N forms in **10** than in **4**−**7**, which is consistent with $^3J_{HH}$ analysis (Table 1). $^3J_{C2',H4'}$ values are slightly larger in **4** and **6** than in **5** and **7** (Table 2), implying a greater preference for S forms in the former, in agreement with $^3J_{HH}$ data (Table 1). However, $^3J_{C2',H4'}$ values are slightly larger in **2** and **3** than in **1**, indicating a similar or slightly greater preference for S forms in the former, whereas $^3J_{C1',H3'}$ values in **1** (5.3 Hz) and in **2** and **3** (∼4.5 Hz) indicate a greater proportion of N forms in solutions of **2** and **3** than **1** (Figure 2), a conclusion consistent with $^3J_{HH}$ data (Table 1) but inconsistent with $^2J_{C2',H4'}$ data. These results suggest that $^3J_{C2',H4'}$ values may not conform to a simple Karplus relationship and may be more difficult to correlate with furanose ring conformation than other $^3J_{CH}$ values (*e.g.*, $^3J_{C1',H3'}$, $^3J_{C1',H4'}$). The computed behavior of $^3J_{C2,H4}$ in β-D-ribofuranose and 2-deoxy-β-D-*erythro*-pentofuranose (2-deoxy-β-D-ribofuranose) (Figure 3) appears to validate these concerns, especially for the latter where the overall change in coupling magnitude as a function of ring conformation is smaller. The presence of two maxima in Figure 3A also reduces the effectiveness of $^3J_{C2',H4'}$ as a conformational probe and complicates its interpretation in the furanose rings of **1**−**7**; similar arguments have been made for $^3J_{H2',H3'}$ in **4**−**7**. This behavior is not observed for other $^3J_{CH}$ values (*e.g.*, $^3J_{C1,H3}$, $^3J_{C1,H4}$) (Figure 3B).

$^3J_{C2',H4'}$ values are, on average, larger in **4**−**7** than in **1**−**3** (Table 2). However, different Karplus equations govern $^3J_{C2',H4'}$ in **1**−**3** and **4**−**7**, since C2′ is not identically substituted in both series of nucleosides. The data suggest that loss of the electronegative oxygen substituent on C2′ results in a decrease in $^3J_{CCCH}$ for a given C2′−C3′−C4′−H4′ dihedral angle. This conclusion is validated by computed coupling data (Figure 3A), at least for dihedral angles of ∼120−150°.

$^3J_{C1',H4'}$ is slightly larger in **1** (2.9 Hz) than in **2** (2.4 Hz) and **3** (2.2 Hz), and should increase as S forms become more favored (Figure 3B). Thus, as suggested from $^3J_{HH}$ (Table 1) and $^3J_{C1',H3'}$

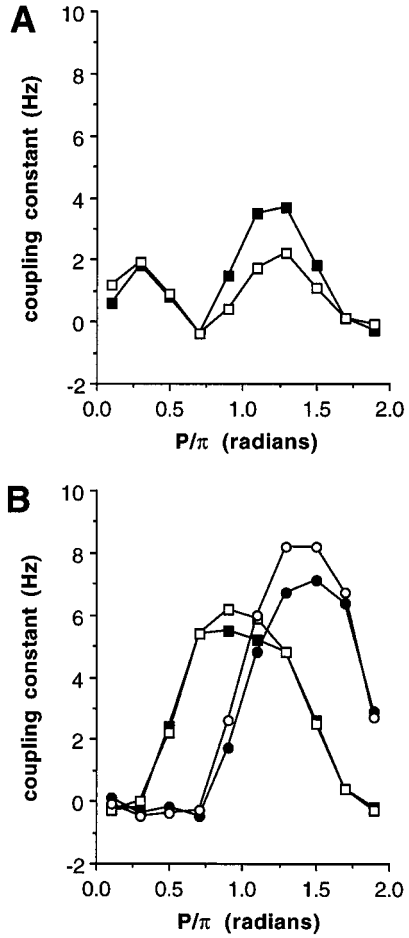

Figure 3. (A) Computed behavior of $^3J_{C2,H4}$ in β-D-ribofuranose and 2-deoxy-β-D-ribofuranose. Solid squares, *ribo*; open squares, deoxy*ribo*. (B) Computed behavior of $^3J_{C1,H3}$ and $^3J_{C1,H4}$ in β-D-ribofuranose and 2-deoxy-β-D-ribofuranose. Solid squares, $^3J_{C1,H3}$ *ribo*; solid circles, $^3J_{C1,H4}$ *ribo*; open squares, $^3J_{C1,H3}$ deoxy*ribo*; open circles, $^3J_{C1,H4}$ deoxy*ribo*.

values (Table 2, see above), $^3J_{C1',H4'}$ data indicate a smaller N/S ratio in purine 2′-deoxyribonucleosides than in pyrimidine 2′-deoxyribonucleosides. In addition, $^3J_{C1',H4'}$ decreases in the conversion of 2′-deoxyribonucleosides to corresponding ribonucleosides (*e.g.*, 2.4 Hz in **2**, 0.6 Hz in **5**), again consistent with a greater preference for N forms in the latter. The larger $^3J_{C1',H4'}$ in **1** (2.9 Hz) relative to **4** (1.3 Hz) (Table 2) suggests a greater preference for S forms by **1**, contrary to PSEUROT data that indicate a similar percentage of S forms in these compounds (Table 1).

E. One-Bond ^{13}C−^{13}C Spin Couplings. $^1J_{C1',C2'}$ in **1**−**3** has been shown previously to be smaller (average, 36.9 ± 0.3 Hz) than $^1J_{C1',C2'}$ in **4**−**7** (average, 42.8 ± 0.2 Hz),[9a] suggesting that the loss of an electronegative substituent on one of the coupled carbons decreases the $^1J_{CC}$ magnitude, in the present case by ∼5.9 Hz. $^1J_{C2',C3'}$ is also smaller in **1**−**3** (average, 35.6 ± 0.1 Hz) than in **4**−**7** (average, 37.8 ± 0.1 Hz), again with the decrease (∼2.2 Hz) attributed to the loss of an electronegative substituent. The extent of the decrease in $^1J_{CC}$ values appears to depend not only on the change in the total number of electronegative substituents on the C−C fragment but also on their distribution. For example, for $^1J_{C1',C2'}$, the total number of substituents changes from three to two in converting **4**−**7** to **1**−**3**, with the latter two residing on one carbon (C1′), whereas for $^1J_{C2',C3'}$, the total number changes from two to one, with the latter residing on one carbon (C3′). Previous studies on ^{13}C-labeled sucrose[30] have shown that $^1J_{CC}$ values decrease by 7−10 Hz upon decreasing the total number of electronegative substituents on the C−C fragment from 3 to 2, with the latter distributed on *both* carbons. Other structural factors may also affect the magnitude of decrease, such as C−C−O−H and HO−C−C−OH torsion angles.[31] Interestingly, $^1J_{C1,C2}$ is 46.1 ± 0.1 Hz in D-glucopyranoses (**15**) and 40.5 ± 0.3 Hz in 2-deoxy-D-glucopyranoses (**16**) (2-deoxy-D-*arabino*-hexopyranoses), giving a difference (5.6 Hz) similar to that observed between **4**−**7** and **1**−**3**, and indicating that substituent rather than conformational factors are the major determinants of the effect.

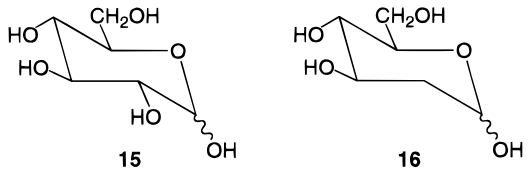

F. Dual-Pathway ^{13}C−^{13}C Spin Couplings. Coupling between C1′ and C3′ in **1** (0.8 Hz) is significantly smaller than the corresponding coupling in **4** (3.3 Hz) (Table 2). This coupling is affected by two pathways (C1′−C2′−C3′ and C1′−O4′−C4′−C3′) and is thus represented as $^{2+3}J_{C1',C3'}$. The observed value of $^{2+3}J_{C1',C3'}$ is assumed to be the algebraic sum of the couplings arising from the two pathways.[32] If a simple two-state N/S exchange between E_2 (N) and ^{2}E (S) is assumed (this model approximates the standard ^{3}E−^{2}E exchange model), then the C1′−O4′−C4′−C3′ torsion angle remains essentially constant at ∼0°, leading to the conclusion that the $^3J_{COCC}$ component cannot be responsible for the different values of $^{2+3}J_{C1',C3'}$ in **1** and **4** (this argument assumes that substituent orientations along the coupling pathway, which differ in N and S forms, have a negligible effect on the ^3J component). The different $^{2+3}J_{C1',C3'}$ values in **1** and **4** must therefore be due to differences in the $^2J_{CCC}$ component, which is affected by two factors: substituent differences (at C2′) and/or conformational change. N/S interconversion (the conformational factor) is not expected to exert a large effect on the $^2J_{CCC}$ component because the *relative* orientations of the two *terminal* electronegative substituents on the C1′−C2′−C3′ fragment are similar in N and S forms (*i.e.*, N1 is quasiaxial and O3′ quasiequatorial in N forms, whereas N1 is quasiequatorial and O3′ quasiaxial in S forms). This factor is a major determinant of $^2J_{CCC}$ in carbohydrates.[33,34ab] We therefore deduce that the substitution change on the intervening C2′ exerts a major influence on the $^2J_{CCC}$ component. Support for this conclusion derives from a comparison of $^2J_{C1,C3}$ values in α- and β-D-glucopyranoses **15** and their 2-deoxy analogs **16**. $^2J_{C1,C3}$ in α-D-glucopyranose is essentially zero, whereas this coupling is −2.3 Hz in 2-deoxy-α-glucopyranose; respective couplings of +4.5 and +1.8 Hz are observed in the β-anomers.[33,34b] These differences cannot be attributed to different solution conformations, because other couplings involving C1, namely, $^2J_{C1,C5}$ and $^3J_{C1,C6}$, are nearly identical in both compounds. Thus, deoxygenation at the

(30) Duker, J. M.; Serianni, A. S. *Carbohydr. Res.* **1993**, *249*, 281−303.
(31) Carmichael, I.; Chipman, D. M.; Podlasek, C. A.; Serianni, A. S. *J. Am. Chem. Soc.* **1993**, *115*, 10863−10870.
(32) Marshall, J. L. *Carbon−Carbon and Carbon−Proton NMR Couplings: Applications to Organic Stereochemistry and Conformational Analysis*, Methods in Stereochemical Analysis; Verlag Chemie International, Deerfield Beach, FL, 1983; Vol. 2, pp 186−193.
(33) King-Morris, M. J.; Serianni, A. S. *J. Am. Chem. Soc.* **1987**, *109*, 3501−3508.
(34) (a) Wu, J.; Bondo, P. B.; Vuorinen, T.; Serianni, A. S. *J. Am. Chem. Soc.* **1992**, *114*, 3499−3505. (b) Church, T.; Serianni, A. S. *Carbohydr. Res.* **1996**, *280*, 177−186.

Chart 3

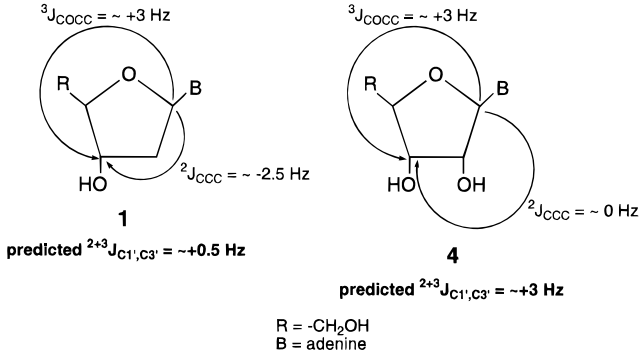

internal carbon along a C−C−C coupling pathway results in a shift to more *negative* couplings (absolute change, ∼−2.5 Hz), which is identical to the change observed in $^{2+3}J_{C1',C3'}$ when converting **4** to **1** (−2.5 Hz; Table 2).

These arguments also lead to a prediction of the sign of $^{2+3}J_{C1',C3'}$ in **4**. Previous studies have shown that $^3J_{COCC}$ values in carbohydrates range from +3.2 to +4.5 Hz for a dihedral angle of ∼180°.[33,34a,b] Thus, a coupling constant of slightly smaller magnitude (∼3 Hz) is expected for a 0° dihedral angle if a conventional Karplus curve is assumed; this $^3J_{COCC}$ component is illustrated in Chart 3. $^2J_{CCC}$ values in carbohydrates are typically small or zero when all three carbons along the coupling pathway are hydroxylated and when only one of the terminal electronegative substituents lies in the C−C−C plane,[33,34a,b] as is the case for both N and S forms of **4**. Thus, the 3.3-Hz coupling observed in **4** is probably positive in sign (+3 Hz + 0 Hz) due to the dominant $^3J_{COCC}$ component (Chart 3). The observed $^{2+3}J_{C1',C3'}$ in **1** is smaller in magnitude (0.8 Hz) because the $^3J_{COCC}$ component remains essentially constant but the $^2J_{CCC}$ component decreases by ∼2.5 Hz (+3 Hz − 2.5 Hz), leading to a small positive coupling (Chart 3). The semiquantitative treatment presented here, however, does not exclude the possibility that $^{2+3}J_{C1',C3'}$ in **1** is negative, given its small absolute value. Experimental confirmation of these predicted signs should be possible via ^{13}C−^{13}C COSY spectra of appropriate triply ^{13}C-labeled **1** and **4**, as described recently.[35]

$^{2+3}J_{C1',C4'}$ in **4**−**7** shows little sensitivity to N/S ratio (Table 2), and thus the small difference between $^{2+3}J_{C1',C4'}$ in **1** and **4** may be due to the different substitution at C2′. Coupling between C2′ and C4′ ($^{2+3}J_{C2',C4'}$) is small or zero in **1**−**3** and only slightly larger in **4**−**8** (Table 2).

G. Three-Bond ^{13}C−^{13}C Spin Couplings. Coupling between C1′ and C5′ is smaller in **1** (0.8 Hz) than in **4** (1.8 Hz) (Table 2). Since this vicinal coupling should be essentially unaffected by structure at C2′, the difference can be attributed to conformational factors. The smaller coupling in **1** relative to **4** is consistent with a higher population of S forms in the former (Table 1), since the C1′−O4′−C4′−C5′ dihedral angle is smaller in S forms than in N forms (Figure 4).

$^3J_{C2',C5'}$ is small or zero in **1**, but 1.3 Hz in **2** and **3**. As shown for $^3J_{C1',C5'}$, the smaller $^3J_{C2',C5'}$ in **1** relative to **2** and **3** is consistent with the former having a larger proportion of S forms in solution (Table 1), since the C2′−C3′−C4′−C5′ dihedral angle is smaller in S forms than in N forms (Figure 4).

H. Other ^{13}C−^{13}C Spin Couplings. In **1**, C2′ is coupled to C8 (1.1 Hz), but no coupling is observed between C2′ and other base carbons. This behavior contrasts with that of C1′, which is coupled to C4 (0.9 Hz), C5 (2.8 Hz), and C8 (2.3 Hz) in **1**.[9a] In **2**, C2′ shows small unresolved couplings to C2 and C6 (observed as broadened signals), whereas in **3**, C2′ is coupled to C6 (1.0 Hz) but not to C2. The small values of $^3J_{C2',C2}$ and $^3J_{C2',C6}$ in **2** and **3** appear consistent with C1′−N1 rotamers containing C2′−C1′−N1−C2 and C2′−C1′−N1−C4 dihedral angles of ∼90°, which occur in a simple two-state *syn* and *anti* exchange model, but these data alone are insufficient to exclude more complex models.

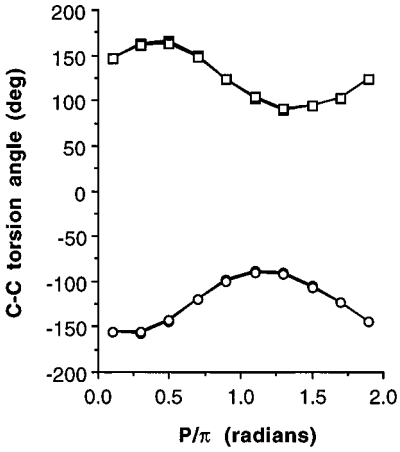

Figure 4. Correlation between furanose ring conformation and C−C torsion angles derived from *ab initio* molecular orbital calculations on β-D-ribofuranose and 2-deoxy-β-D-ribofuranose. Solid squares, C1−C5 *ribo*; solid circles, C2−C5 *ribo*; open squares, C1−C5 deoxy*ribo*; open circles, C2−C5 deoxy*ribo*.

Conclusions

Recent investigations[9a,10,15a,16a] have demonstrated that J_{CH} and J_{CC} values in nucleosides may provide valuable information on the structure and conformation of these compounds in solution. In the present study, spin-coupling constants involving C2′ in 2′-deoxyribonucleosides have been measured and interpreted with assistance from $^3J_{HH}$ data and coupling data involving other furanose ring carbons. This integrated approach allows for an assessment of the degree of internal consistency of conformational conclusions based on different couplings that are affected by similar structural features.

While this study has focused on the behavior of ^{13}C−^{1}H and ^{13}C−^{13}C spin-coupling constants in simple ribonucleosides **4**−**7** and 2′-deoxyribonucleosides **1**−**3**, it is expected that J_{CH} and J_{CC} values will also be valuable in conformational studies of oligonucleotides. This investigation utilized 2D TOCSY methods to obtain J_{CH} sign information only, since accurate coupling magnitudes could be extracted from 1D ^{1}H spectra with good precision (±0.1 Hz). However, recent investigations have shown that accurate J_{CH} values can be measured in RNA oligomers using E.COSY methods;[36,37] in a 19-mer, ^{13}C−^{1}H spin couplings as small as 0.2 Hz have been reported,[37] thus providing evidence that the small $^2J_{CH}$ and $^3J_{CH}$ values observed in **1**−**7** may be applied to studies of larger structures. While longer range J_{CC} values have not been explored in RNA and DNA oligomers, the quantitative *J* correlation method[38] has been used recently to measure $^3J_{CC}$ values in small proteins (<∼3 Hz),[39] thus leading to the expectation that similar measurements might be feasible in oligonucleotides.

(35) Serianni, A. S.; Bondo, P. B.; Zajicek, J. *J. Magn. Reson. Ser. B* **1996**, *112*, 69−74.

(36) Hines, J. V.; Landry, S. M.; Varani, G.; Tinoco, I., Jr. *J. Am. Chem. Soc.* **1994**, *116*, 5823−5831.

(37) Marino, J. P.; Schwalbe, H.; Glaser, S. J.; Griesinger, C. *J. Am. Chem. Soc.* **1996**, *118*, 4388−4395.

(38) (a) Grzesiek, S.; Vuister, G. W.; Bax, A. *J. Biomol. NMR* **1993**, *3*, 487−493. (b) Bax, A.; Max, D.; Zax, D. *J. Am. Chem. Soc.* **1994**, *114*, 6924−6925.

(39) Hu, J.-S.; Bax, A. *J. Am. Chem. Soc.* **1996**, *118*, 8170−8171.

One-bond $^{13}C-^{1}H$ spin couplings involving C2′ in **1**−**3** behave as expected based on recent correlations with C−H bond orientation in solution.[16a,24] Coupling-structure correlations indicate that $^{1}J_{C1',H1'}$ in **1**−**7** may be more sensitive to changes in C1−H1 bond length/orientation than to other factors such as *N*-glycoside torsion.[10]

A key problem in the interpretation of $^{2}J_{CCH}$ values in **1**−**7** involving C1′ and C2′ is the effect of *N*-substitution on their magnitudes and signs. Previous studies of carbohydrates have yielded a general method (projection rule[25c]) to predict $^{2}J_{CCH}$ values when oxygen substitution occurs at one or both carbons along the coupling pathway. This rule cannot be applied to interpret $^{2}J_{C2',H1'}$ in nucleosides due to the presence of *N*-substitution along the coupling pathway;[15a] interestingly, however, the projection rule does allow for a reasonable analysis of $^{2}J_{C1',H2'}$ values.[15a] Using experimental and computational methods, this behavior has been confirmed in the present study, leading to a modified projection rule appropriate for $^{2}J_{C2',H1'}$. Results also show that N/S interconversion will exert different effects on related $^{2}J_{CH}$ values in ribo- and 2′-deoxyribonucleosides (*e.g.*, $^{2}J_{C2',H3'}$ in **4**−**7** is sensitive to N/S exchange but $^{2}J_{C2',H3'}$ in **1**−**3** is not).

$^{3}J_{C2',H4'}$ values in **1**−**3** do not appear to respond to changes in molecular dihedral angles as expected based on classical Karplus relationships,[40] in contrast with the behavior of $^{3}J_{C1',H3'}$ values in **1**−**7**. This behavior will require further study, but present data indicate a need for caution when interpreting $^{3}J_{CH}$ values in **1**−**7** in the absence of appropriate Karplus curves for the coupling pathways under consideration.

$^{13}C-^{13}C$ spin couplings in **1**−**7** have not been well studied.[9a,10] This report attempts to apply correlations observed previously in carbohydrates[31,33,34a,b] to interpret the magnitudes of $^{1}J_{CC}$, $^{2}J_{CC}$, and $^{3}J_{CC}$ values in nucleosides. Comparisons between **1**−**3** and **4**−**7** show the expected effect of electronegative substituents on $^{1}J_{CC}$ values.[41] On the other hand, $^{2}J_{CC}$ values *within* the furanose ring are more difficult to assess due to the dual-pathway problem.[32] However, an application of empirical coupling−structure correlations and couplings obtained from model compounds leads to the conclusion that the different values of $^{2}J_{C1',C3'}$ observed in **1**−**3** and **4**−**7** are due to differences in structure at C2′ and not to conformational factors. Only two $^{3}J_{CC}$ values exist in **1**−**7** ($^{3}J_{C1',C5'}$ and $^{3}J_{C2',C5'}$) and both appear to depend on dihedral angle θ (*e.g.*, C1′−O5′−C4′−C5′ and C2′−C3′−C4′−C5′, respectively) as expected for vicinal couplings (Karplus relationship), although the precise form of their dependence remains to be established.

Acknowledgment. The research reported herein was supported by the Office of Basic Energy Sciences of the United States Department of Energy and Omicron Biochemicals, Inc. of South Bend, IN. This is Document No. NDRL-3933 from the Notre Dame Radiation Laboratory.

JA961622G

(40) (a) Schwarcz, J. A.; Perlin, A. S. *Can. J. Chem.* **1972**, *50*, 3667−3676. (b) Spoormaker, T.; de Bie, M. J. A. *Recl. Trav. Chim. Pays-Bas* **1978**, *97*, 85−87.

(41) Krivdin, L. B.; Kalabin, G. A. *Prog. NMR Spectrosc.* **1989**, *21*, 293−448.